# SALT WEATHERING BY SULFATES: INFLUENCE OF SALINE SOLUTION PROPERTIES

E. Ruiz-Agudo y C. Rodríguez-Navarro

*Dept. Mineralogía y Petrología, Universidad de Granada, Fuentenueva s/n, 18002 Granada, Spain.*

## INTRODUCTION

The crystallization of soluble salts in porous materials is one of the major causes rock decay in nature (e.g., arid and desert regions, coastal areas, Antarctica –Evans, 1970; Winkler and Singer, 1972) and weathering of stone buildings and other engineering structures (Winkler, 1994; Goudie et al. 1997; Rodriguez-Navarro and Doehne, 1999). The growth of a crystal in a confined space (pore) can exert a pressure sufficient to exceed the rupture modulus of most ornamental materials, including stone, mortars and bricks, causing their breakage. It is therefore important to know the mechanisms of damage and the parameters controlling the process of salt weathering as a first step to design methods to mitigate this problem in the fields of civil engineering and cultural heritage conservation. Here we have studied differences in crystallization behavior of sodium and magnesium sulfates. These two salts are extensively found in both new cement structures and porous building stones. Both are extremely damaging and show completely different crystallization patterns; however, their damage mechanism has not yet been clarified. Our study reveals some keys parameters which control salt damage of porous stone, such as where crystallization occurs and in what kind of pores in the case of each salt are ultimately determined by pore size distribution of stone and salt solution properties. These results may help elucidate why these salts are so damaging, which is critical to designing possible solutions to reduce damage caused by such sulfates.

## MATERIALS AND METHODS

### Studied salts

The $Na_2SO_4$-$H_2O$ system includes two stable phases: thenardite ($Na_2SO_4$), the anhydrous phase that precipitates directly from solution at temperatures above 32.4°C, and mirabilite ($Na_2SO_4 \cdot 10H_2O$), the stable phase below this temperature. Mirabilite dehydrates to thenardite at RH below 71 % (20 ºC). Sodium sulfate heptahydrate ($Na_2SO_4 \cdot 7H_2O$) has been described as precipitating at temperatures below the mirabilite/thenardite transition point. However, this phase is metastable and has not been clearly identified in nature. On the other hand, the only naturally occurring members of the $MgSO_4 \cdot nH_2O$ series on Earth are epsomite ($MgSO_4 \cdot 7H_2O$, 51 wt% water), hexahydrite ($MgSO_4 \cdot 6H_2O$, 47 wt% water) and kieserite ($MgSO_4 \cdot H_2O$, 13 wt% water). Epsomite transforms readily to hexahydrite by loss of extra-polyhedral water; this transition is reversible and occurs at 50–55% relative humidity (RH) at 298 K and at lower temperatures as the activity of water diminishes (Vaniman et al., 2004). Both magnesium and sodium sulfates are used for stone accelerated decay testing because their crystallization is highly damaging (ASTM 1997; Rodriguez-Navarro and Doehne, 1999).

### Stone characterization

The damaging effects of salt crystallization within a natural porous medium were studied using a biomicritic limestone (calcarenite). The calcarenite was quarried in the Santa Pudia area (15 km SW from Granada). It is buff colored, quite porous and easy to quarry and carve. These characteristics led to its extensive use in the Andalusian's architectural and sculptural heritage. It has well-known salt weathering problems. The calcarenite overall porosity, determined by mercury intrusion porosimetry (MIP), is 32.2 %, with a mean pore radius of 13.5 μm. Calcarenite pore size distribution graphs (Fig. 3) show abundant macropores, with a mean pore radius of ca. 30 μm. Smaller pores are also detected with secondary

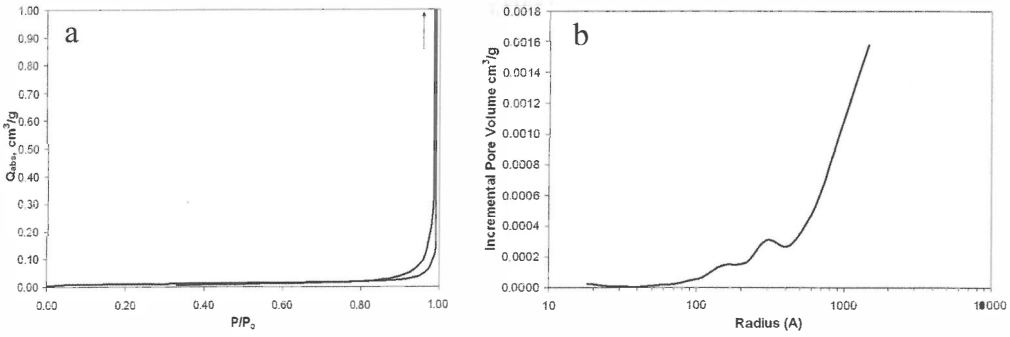


*Figure 1: $N_2$ sorption isotherms (a) and BJH pore size distribution (b) of Santa Pudia's limestone*

| | $W(t)_{max}$, % | $W(t)_{abs}$, % | $I_m$, % | $V_{abs}$, %/$h^{1/2}$ | $V_{des}$, %/$h^{1/2}$ | $V_{cap}$, cm/$h^{1/2}$ | $C_{suc}$, g/$cm^2h^{1/2}$ |
|---|---|---|---|---|---|---|---|
| *Limestone* | 19.14 | 14.70 | 23.17 | 6.39 | 3.71 | 12.9 | 2.75 |

*W(t)max: maximum water content (saturation); W(t)abs: maximum water content (absorption);; Im: microporosity index; Vabs: absorption velocity; Vdes: desorption velocity; Vcap: capillary suction velocity;; Csucc: capillary suction coefficient*

*Table 1: Hydric characteristics of Santa Pudia's Limestone (from Rodríguez-Navarro, 1994)*

maxima at ca. 0.1 μm. The calcarenite shows a small specific surface area (0.815 $m^2/g$, according to the BET method). The nitrogen absorption isotherm (Fig. 1a) is of type III, typical of non-microporous solids. The BJH plot (Fig. 1b) shows the presence of a significant amount of meso and macropores (pore radius > 50 nm). Hydric properties are summarized in Table 1 (Rodriguez-Navarro, 1994).

### Macroscale salt crystallization experiments

Saturated salt solutions were prepared from crystalline solid (Panreac, analytical grade) using deionized water, filtered and heated to eliminate any undissolved salt crystals. Salt crystallization tests were carried out in a controlled environment (20±2ºC, and 45±5% relative humidity). The solutions were let to flow-through, evaporate and crystallize in the porous stone (Fig. 2). See Rodriguez-Navarro et al. (2002) for details on the laboratory set-up. The solution evaporation rate was measured by continuous weighing of the stone–solution–beaker system. Salt crystals grown within the stone, as well as on its surface (efflorescence) were collected after crystallization experiments and examined by powder X-ray diffraction (XRD) and environmental scanning microscopy (ESEM) with no prior treatment (i.e., no grinding) in order to infer their growth morphology.

## RESULTS AND DISCUSSION

Porosity and pore size distribution are key factors controlling the uptake and transport of liquid within a stone (Rodriguez-Navarro and Doehne, 1999). Stones such as Santa Pudia's limestone with a high proportion of mesopores connected to large pores are very susceptible to salt weathering. These mesopores result in larger surface area for evaporation and slower solution transport, thus increasing the chances that high supersaturation ratios will be reached below the stone surface (subflorescence growth). In stones with larger pores, capillary rise is limited, surface area is lower, and solutions readily reach the stone surface, without achieving a high supersaturation, thus resulting in efflorescence growth.

Hydric properties (Table 1) show that the calcarenite rapidly absorbs water, but dries slow. Thus, salt solutions will be taken up fast, but will remain within the stone pore system for enough time to precipitate as harmful subflorescence. Such behavior contributes to the overall susceptibility of this stone towards salt weathering. Crystallization of both Na sulfate and Mg sulfate reduce the stone porosity (29.5 and 24.2 %, respectively) and mean pore radius (3.1 and 6.4 μm, respectively). Na sulfate induces the deposition of crystals within the bigger pores of the stone (Fig. 3a), close to the surface, forming thin stone surface layers that lift up successively (Fig. 4b). ESEM analysis of salt crystals grown in stone slabs show direct precipitation of thenardite with bow-tie

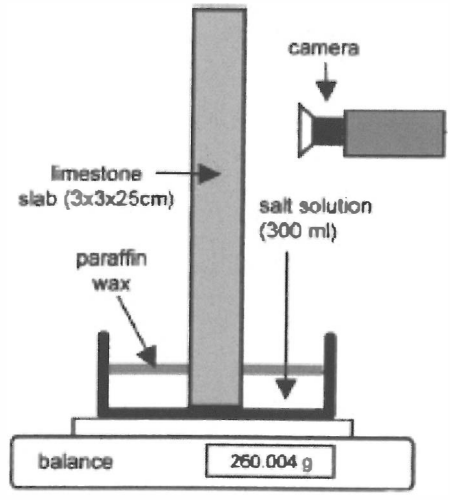


*Figure 2: Laboratory set-up for crystallization experiments*

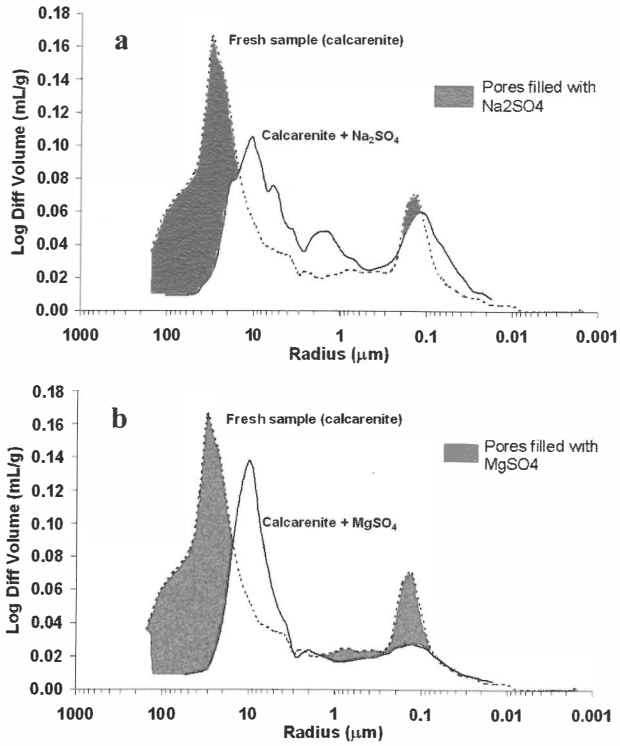


*Figure 3: MIP pore size distribution of limestone before and after crystallization of Na sulfate (a) and Mg sulfate (b)*

morphology (Fig. 5a). Note that if mirabilite would have been precipitated first, and subsequently dehydrated, a porous crystal retaining mirabilite bulk shape would have formed. The observed morphology of thenardite is typical of crystallization at a high supersaturation (Sunawaga, 1981). The crystals thus generate high crystallization pressure and cause significant damage. Heterogeneous nucleation of $Na_2SO_4$ over calcite minerals in a limestone

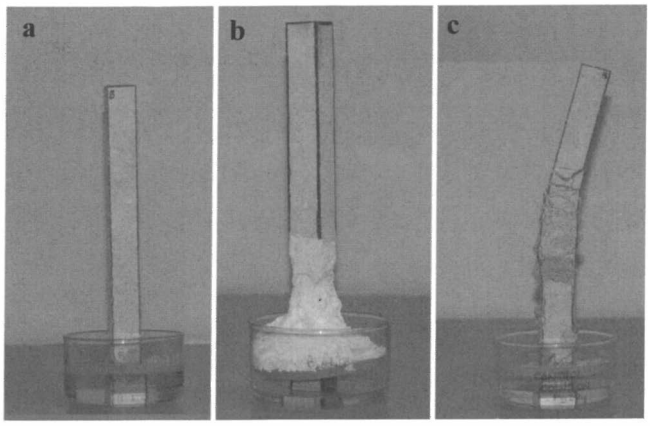


*Figure 4: Sulfate damage in limestone slabs: a) before crystallization tests; b) after sodium sulfate crystallization and c) after magnesium sulfate crystallization.*

pore may induce thenardite precipitation and growth at temperatures below 32.4 ºC (Rodriguez-Navarro and Doehne, 2000). In contrast, Mg sulfate shows a decay mechanism based on crack propagation (Fig. 4c). Epsomite precipitates deep into the limestone, filling large and small pores (Fig. 3b), with crystals displaying near equilibrium forms (Fig. 5b). This was also observed by Rodriguez-Navarro and Doehne (1999) in the case of halite formed within limestone.

These results disagree with the generally accepted Wellman and Wilson (1965) theory for salt crystallization.

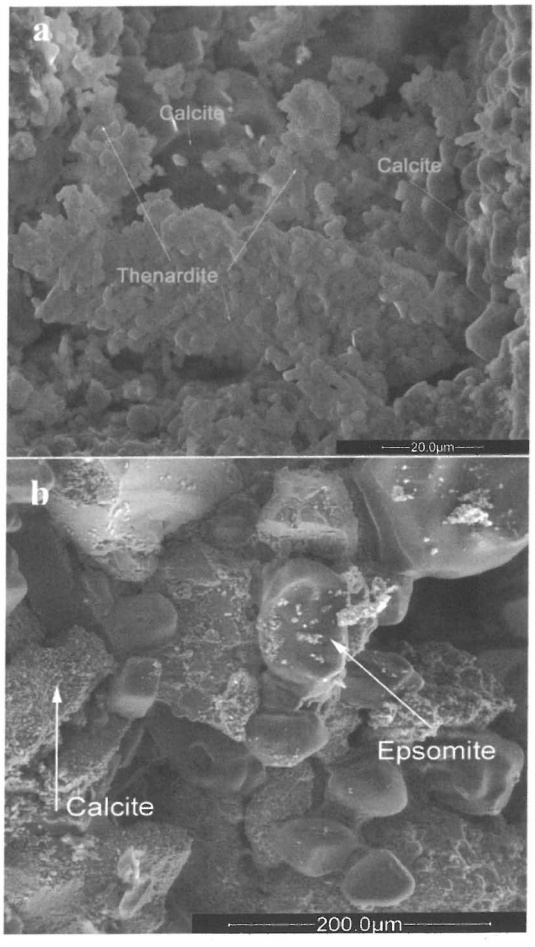


*Figure 5: ESEM micrographs of sulfates growing in limestone pores: a) Na sulfate and b) Mg sulfate.*

| Saturated solution | Concentration ( g anhyd./100 g $H_2O$) | Density ($g/cm^3$) | Surface Tension (mN/m) | Viscosity (cP) | Vapor Pressure (kPa) |
|---|---|---|---|---|---|
| $Na_2SO_4$ | 19.4 | 1.15 | 75.45 | 1.834 | 2.175 |
| $MgSO_4$ | 33.5 | 1.29 | 77.35 | 7.270 | 2.781 |

*Table 2: Physical properties of salt solutions used in crystallization experiments (20ºC).*

According to this theory, the crystal/saturated solution surface free energy is higher in smaller pores than in coarser ones because of volume constraints. Thus salt crystallization is thermodynamically not favorable in small pores. However, it has to be taken into account that ionic transport in porous materials is a competition between salt advection to the evaporation front, and ion diffusion (Pel, 2002). Drying rate is the key parameter that controls the prevalence of one mechanism or the other. If the drying is slow, diffusion controls the process (Rijniers, 2004). As water evaporates in large pores, ions are transported to small pores where the concentration is lower. Finally, crystallization takes place in both large and small pores at a very high supersaturation, thus leading to important damage. This is the case of Mg sulfate. If the drying is very fast, salt is transported by advection to the position where evaporation takes place and salts precipitate, that is to say, in large pores. This behavior was observed in the case of Na sulfate.

Ultimately, the physical properties of a saline solution (i.e., viscosity, density, surface tension and vapor pressure) will control the dynamics of solution flow and evaporation within the porous network of the stone (since environmental conditions were kept constant in our tests), and therefore the dynamics of precipitation and salt growth and the resulting damage to porous substrate. Flow is governed by Poseuille's law, where the driving force is capillary pressure (Lewin, 1982). The differential flow behavior of the two saline solutions is mainly due to the differences in viscosity (Table 2). Due to its higher viscosity, capillary flow is slower in the case of saturated magnesium sulfate solution (compared with that of sodium sulfate solution at the RH and T of the experiment). As a consequence, evaporation occurs faster than the replenishment of the solution by capillary migration from the inside of the stone, and precipitation takes place under the stone surface. The drying-out of solution within a pore opening at the surface occurs by diffusion of water vapor through a layer of the porous solid, and is governed by Fick's law. Once the solution

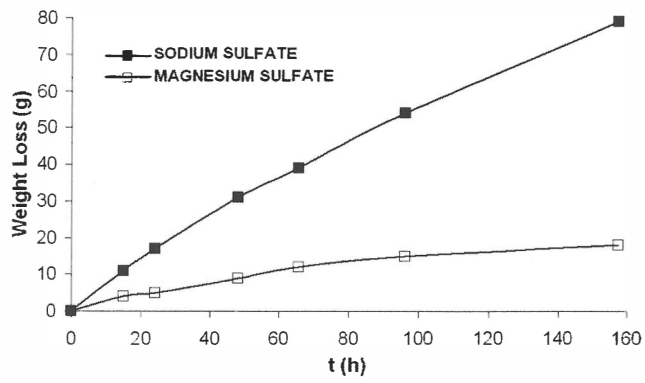


*Figure 6: Evaporation rate of sodium sulfate and magnesium sulfate saline solutions from limestone slab.*

reaches the evaporation front it would be expected that the evaporation rate will be faster in the case of magnesium sulfate, as its vapor pressure is higher (the evaporation rate increases with vapor pressure). However, due to the fact that the evaporation front is placed inner in the stone (compared with sodium sulfate) the rate of water vapor diffusion and, finally, the effective evaporation rate, would be much lower (Fig. 6).

## CONCLUSIONS

Both Na and Mg sulfate are extremely damaging salts, as has been observed in field and laboratory tests. While the mechanism of salt weathering by Na sulfate consists in the detaching of successive stone layers, Mg sulfate induces crack formation and propagation within the bulk stone. Differential damage created by Na sulfate and Mg sulfate is mainly due to differences in their crystallization pattern since we kept constant the environment variables (RH and T) and the porous support (Santa Pudia's limestone). The physical properties of the salt solution, i.e. density, surface tension, and, in particular, viscosity, have a critical effect on the dynamics of solution flow and evaporation within the stone, and therefore, on where crystallization occurs and in what kind of pores, as well as on the resulting damage to porous host materials. High flow rates lead to crystallization inside the stone in coarse pores. As a result of low flow rates within the porous network, crystallization takes place inside the stone in both small and big pores. Crystallization on stone surface as efflorescence would avoid/minimize stone damage due to salt crystallization. This can be achieved by acting not only on the crystallization process (i.e., increasing induction times by the addition of crystallization inhibitors), but also in the solution transport process within the stone (i.e., high flow rates), as they both play a crucial role in salt damage. The use of compounds (such as surfactants) that influence salt crystallization pattern by modifying transport/flow properties of saline solutions inside porous materials may reduce salt damage in such building materials. This proposed treatment could enhance the effect of other methods that act mainly modifying the crystallization process (i.e., crystallization inhibitors).

## ACKNOWLEDGEMENT

This work has been financially supported by the European Commission VIth Framework Program, under Contract no. SSP1-CT-2003-501571, and the research group NRM-179 (Junta de Andalucía, Spain).

## REFERENCES

ASTM C 88-90 (1997) ASTM Annual Book of Standards, 4.2, 37- 42.

Evans, I. S. (1970) Rev. Geomorphologie Dynamique, 19, 153-177.

Goudie, A. S., Viles, H.A.; Parker, A. G. J. Arid Environm. 1997, 37, 581-598

Lewin, S.Z. (1982) In: «Conservation of Historic Stone Buildings and Monuments», N.S. Baer, ed. National Academy Press, 120-162.

Pel, L. (2002). Appl. Phys. Lett., 81(15), 2893-2895.

Rijniers, L. (2004) PhD dissertation, Techniche Universiteit Eindhoven, 112 pp.

Rodriguez-Navarro, C. (1994) PhD dissertation, University of Granada, 412 pp.

Rodriguez-Navarro, C. and Doehne, E. (1999) Earth Surface Processes Landforms, 24, 191-209.

Rodriguez-Navarro, C. and Doehne, E. (2000) Cement Concrete Res., 30, 1527-1534.

Rodriguez-Navarro, C.; Linares-Fernandez, L.; Doehne, E. and Sebastian-Pardo, E. (2002) J. Cryst. Growth, 243, 503–516.

Sunagawa, I. (1981) Bull. Mineralogy, 104 ,81-87.

Vaniman, D.T.; Bish, D.L.; Chipera, S.J.; Fialips, C.I.; William Carey, J.; Feldman, W.C. (2004) Nature, 431, 663-665.

Wellman, H. W. and Wilson, A.T. (1965). Nature, 205, 1097-1098.

Winkler, E. M.; Singer, P. C. (1972) Geol. Soc. Am. Bull., 83(11), 3509-13.

Winkler, E.M. (1994) Stone in Architecture, Properties and Durability. Springer-Verlag, Berlin, 313 pp.